Reversing the Chemoselectivity in Photocatalytic C–F Bond Cleavage Enabled by Zirconocene and Photoredox Catalysis

Haruki Takimoto,[a] Kazuhiro Aida,[a] Yoshio Nishimoto,[b]* Daisuke Yokogawa,[c] Eisuke Ota,[d]* Junichiro Yamaguchi[a]*

[a] Department of Applied Chemistry, Waseda University, 513 Wasedatsurumakicho, Shinjuku, Tokyo 162-0041, Japan.

[b] Graduate School of Science, Kyoto University, Kyoto 606-8502, Japan.

[c] Graduate School of Arts and Sciences, The University of Tokyo, 3-8-1 Komaba, Meguro-ku, Tokyo 153-8902, Japan.

[d] Waseda Institute for Advanced Study, Waseda University, 513 Wasedatsurumakicho, Shinjuku, Tokyo 162-0041, Japan.

Zirconocene, Photoredox catalyst, Defluorination, Halogen atom transfer, α-fluoroacetate

ABSTRACT: The development of chemoselective defluorination reactions is highly desirable due to the exceptional stability of the C–F bond compared to other functional groups. Recent advances in photocatalysis have enabled catalytic single-electron transfer (SET) processes, offering an alternative to stoichiometric methods that rely on strong reducing agents. However, these strategies have primarily focused on trifluoromethyl substrates, with limited success for compounds containing fewer fluorine atoms, which are inherently more resistant to SET. Herein, we report a novel defluorination strategy for α-fluorocarbonyl compounds, employing zirconocene and photoredox catalysis. Our method leverages the strong fluorine affinity of zirconocene and bypassed reliance on reduction potential, focusing instead on the bond dissociation energy of the fluorinated molecules. This methodology offers a complementary approach for catalytic C–F bond cleavage under visible-light conditions.

INTRODUCTION

Bond cleavage reactions play a fundamental role in organic synthesis, enabling the generation of reactive intermediates crucial for subsequent synthetic steps. Selective bond cleavage is essential for the efficient production of target molecules while minimizing undesired side reactions. As a result, there is growing demand for novel methodologies that enable the chemoselective cleavage of inert bonds in the presence of more reactive functional groups.

Among these, the C*sp*^{3}–F bond stands as one of the strongest single bonds in organic molecules.[1,2] While various defluorination methods have been developed–including base-mediated, transition metal-catalyzed and Lewis acid catalyzed approaches[3–14]–recent advances in photoredox chemistry have brought significant progress to this field. However, these photoredox-catalyzed methods have predominantly focused on trifluoromethyl-substituted arenes and trifluoroacetic acid derivatives, utilizing potent reductants, such as excited-state transition metal complexes,[15–21] CO_2 radical anions, or photoexcited organic catalysts.[22–43] (Figure 1A).

This focus is understandable, as the relatively positive reduction potentials of trifluoromethyl arenes (–1.8 V vs SCE)[34] and trifluoroacetic acid derivatives (–2.0 V vs SCE)[38] make them more accessible to single-electron transfer (SET)-based strategies (Figure 1B). However, as the number of fluorine decreases, the reduction potential similarly becomes more negative, rendering monofluorinated compounds particularly challenging substrates for SET-based methods. Despite the vast number of methods for trifluoromethyl compounds, efficient photocatalytic methodologies for the (multiple)defluorination of monofluoromethyl compounds remain elusive, being limited to carboxylation[37] and hydrogenation (or deuteration).[31,36] Particularly, only hydrogenation of acetanilide has been reported for monofluoroacetate derivatives.[31] Developing chemoselective cleavage methods targeting the monofluoromethyl group, even in the presence of trifluoromethyl group, would significantly enhance the synthetic utility of photocatalytic C–F bond cleavage strategies.

In contrast, the bond dissociation energy (BDE) of the C–F bond decreases in the order CF_3>CF_2H>CFH_2 (Figure 1B).[44] Thus, the development of novel defluorination reactions based on the BDE rather than reduction potential could reverse chemoselectivity, and offer direct access to monofluorinated compounds. This approach would provide a complementary strategy to most current visible-light driven C–F bond activation methods.

Halogen atom transfer (XAT) is one example of a reaction that primarily depends on BDE.[45–47] Recent advancements in visible-light-mediated XAT have enabled the use of even unactivated alkyl chlorides as radical precursors, using various radical species such as α-aminoalkyl radicals,[48–53] silyl radicals,[54–67] ligated boryl radicals,[68–71] γ-terpinenyl

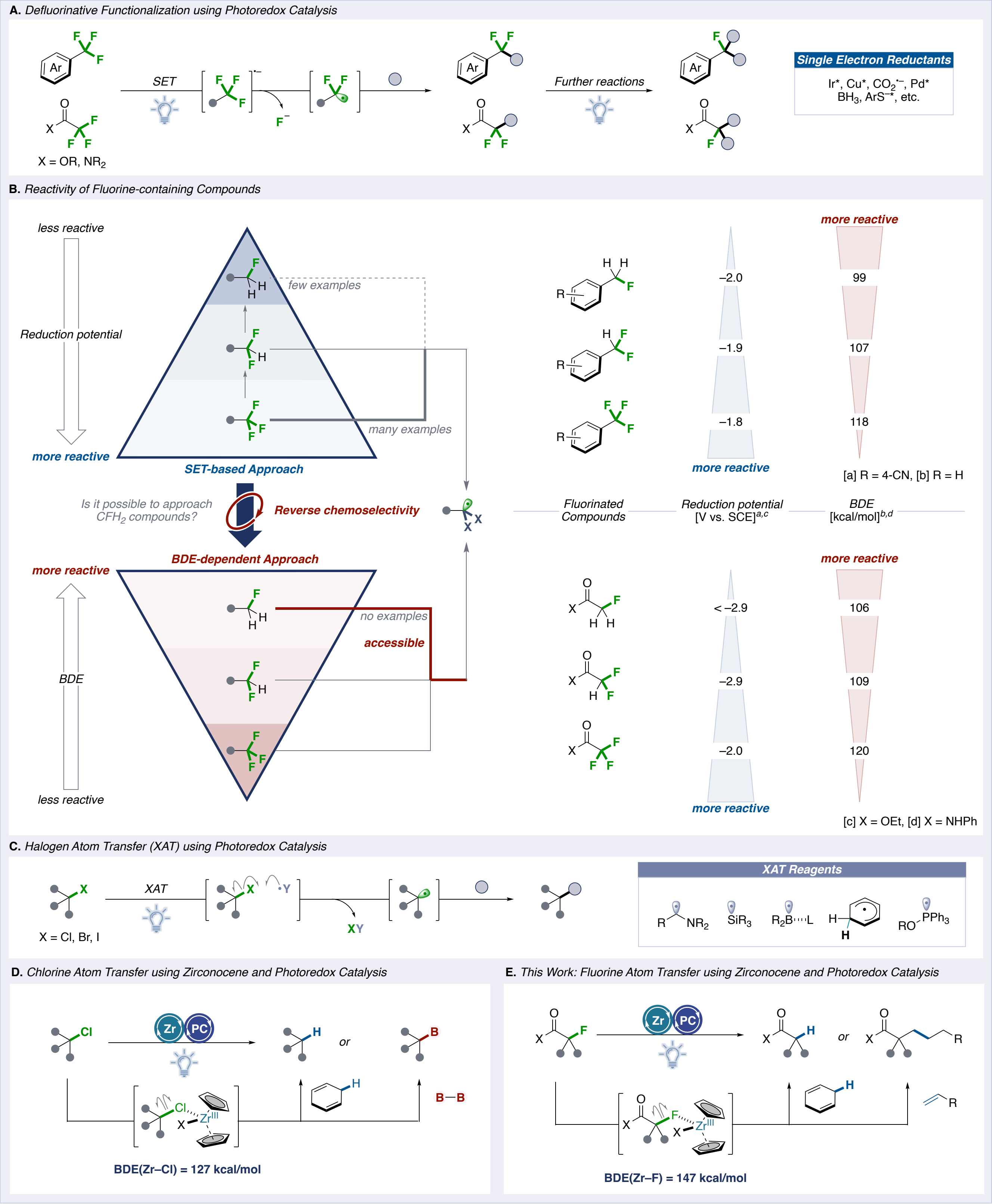

Figure 1. (A) Defluorinative functionalization reactions using photoredox catalysis. (B) Reactivity of fluorine-containing compounds arising from their redox potential and bond dissociation energy. (C) Halogen atom transfer (XAT) using photoredox catalysis. (D) Dechlorination of alkyl chloride using zirconocene and photoredox catalysis. (E) This work: defluorinative hydrogenation and alkylation of α-fluoro carbonyl compounds.

radicals,[72] and phosphoranyl radicals[73] (Figure 1C). However, fluorine atom abstraction, due to the high BDE value of the C–F bond, has seen limited success and restricted to perfluoro compounds.[18,74,75] Developing XAT-based methods for monofluoromethyl compounds would not only expand the XAT field but also offer a new activation platform with distinct chemoselectivity for C–F bond cleavage compared to SET-based approaches.

Recently, our group developed a dechlorination reaction using zirconocene and photoredox catalysis (Figure 1D).[76] In this system, $\mathrm{Zr^{III}}$, generated by the reduction of $\mathrm{Zr^{IV}}$ by an excited photocatalyst, abstracts a chlorine atom from alkyl chlorides, driven by the formation of the strong Zr–Cl bond (BDE(Zr–Cl) = 127 kcal/mol).[44] Building on this success and earlier reports of C–F bond cleavage by zirconocenes,[77,78] we hypothesized that our catalytic platform could be extended to fluorine atom transfer, exploiting the strong fluorine affinity of $\mathrm{Zr^{III}}$ (BDE(Zr–F) = 147 kcal/mol).[44] Herein, we report a new catalytic platform for fluorine atom transfer using zirconocene and photoredox catalysis, successfully applied to mainly monofluorocabonyls, which have thus far been inaccessible for visible-light-driven defluorinative functionalization due to their highly negative reduction potentials (< –2.9 V SCE) (Figure 1E).

RESULTS AND DISCUSSION

Based on our hypothesis, we initially investigated the reaction conditions using *n*-butyl α-fluoroacetate (**1a**) as a model substrate (Table 1). Gratifyingly, in the presence of Ir(4-*t*Buppy)$_3$, (^{n}BuC$_5$H$_4$)$_2$ZrCl$_2$, 1,3-dimethyl thiourea, and γ-terpinene, visible light irradiation of **1a** afforded the defluorinated compound **2a** in 89% yield (entry 1). However, using Cp$_2$ZrCl$_2$ led to a reduced yield of **2a**, and significantly lower conversion was observed with Cp*$_2$ZrCl$_2$ (entries 2 and 3). This is consistent with the difficulty in reducing Cp*$_2$ZrCl$_2$ (E_{red} = –2.08 V vs. SCE).[79] Next, we evaluated the effect of thiourea substituents. While dialkyl thioureas (**TU2**) provided good yields of **2a** (entry 4), diphenyl thiourea (**TU3**) was ineffective in promoting the reaction (entry 6). The use of **TU4** also failed to yield the desired product **2a**, suggesting that the N–H bond plays a crucial role in the reaction efficiency. Although the reaction proceeded in the absence of thiourea additive, the yield of **2a** was decreased significantly (entry 7).

Interestingly, applying the reaction conditions previously established for the dechlorination (5.0 mol% Cp$_2$Zr(OTs)$_2$, 3.0 mol% Ir(4-MeOppy)$_3$, 60 mol% 1,3-di(p-tolyl)thiourea, 1,4-CHD (3.0 equiv), PhCF$_3$, MS4Å, blue LEDs, 35 °C, 12 h) did not promote defluorination. This indicates that the defluorination requires a distinct set of conditions compared to dechlorination. However, after further optimization of these parameters, we identified effective reaction conditions for this transformation. Additional screening of photocatalysts and solvents also influenced the yield of **2a** (see the Supporting Information for details). Control experiments in the absence of photocatalyst, zirconocene, or visible light irradiation resulted in no product (entries 8–10), highlighting the essential role of each component and the necessity of visible light.

Table 1. Reaction optimization[a]

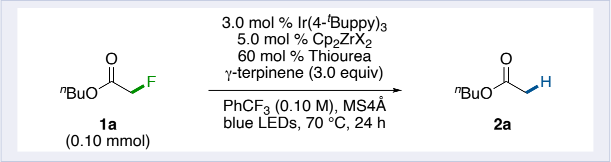

entry	Cp$_2$ZrX$_2$	thiourea	Yield of **2a** /%
1	(^{n}BuC$_5$H$_4$)$_2$ZrCl$_2$	**TU1**	89
2	Cp$_2$ZrCl$_2$	**TU1**	64
3	Cp*$_2$ZrCl$_2$	**TU1**	3
4	(^{n}BuC$_5$H$_4$)$_2$ZrCl$_2$	**TU2**	70
5	(^{n}BuC$_5$H$_4$)$_2$ZrCl$_2$	**TU3**	40
6	(^{n}BuC$_5$H$_4$)$_2$ZrCl$_2$	**TU4**	18
7	(^{n}BuC$_5$H$_4$)$_2$ZrCl$_2$	none	43
8[b]	(^{n}BuC$_5$H$_4$)$_2$ZrCl$_2$	**TU1**	0
9	none	**TU1**	0
10[c]	(^{n}BuC$_5$H$_4$)$_2$ZrCl$_2$	**TU1**	0

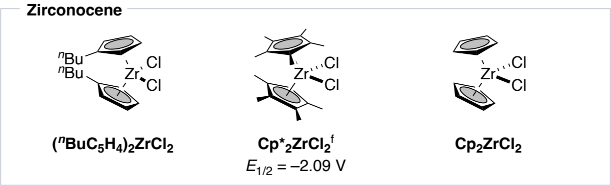

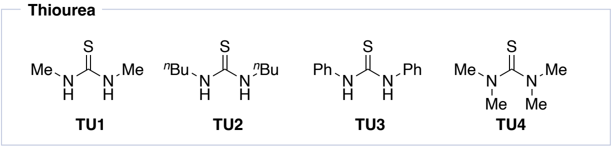

[a]Conditions: **1A** (0.10 mmol), 3.0 mol % Ir(4-*t*Buppy)$_3$, 5.0 mol % Cp$_2$ZrX$_2$, 60 mol % thiourea, γ-terpinene (3.0 equiv), solvent (1.0 mL), 456 nm LEDs (Kessil® lamp), 70 °C, 24 h. [b]without photocatalyst. [c]without irradiation.

With the optimized reaction conditions, in hand, we next explored the substrate scope (Table 2). Various α-fluoroacetic acid derivatives, including alkyl ester (**1a**), benzyl esters (**1b–1e**), benzyl amide (**1f**), and anilides (**1g** and **1h**), were successfully defluorinated, affording to the corresponding hydrogenated products **2a–2h** in moderate to good yields. Interestingly, the starting material to anilide **2g**, monofluoromethyl compound **1g**, is the product of a SET-based photoredox reaction that typically targets trifluoromethylated compounds.[6] This observation highlights the complementary nature of the newly developed reaction compared to SET-based photoredox processes. Notably, defluorination occurred preferentially over the dehalogenation of bromoarenes ($E_{1/2}$ = –2.2 V vs SCE)[80] or chloroarenes ($E_{1/2}$ = –2.6 V vs SCE),[80] which are more susceptible to single-electron reduction. Additionally, benzyl fluoride (**1i**) and difluoroacetamide (**1j**), which possess weaker (97.6 kcal/mol)[44] and similarly strong C–F bonds, respectively, compared to monofluoroacetate, were also successfully defluorinated. Secondary alkyl fluorides, including easily reducible substrates such as ketone (**1k**) and trifluoromethyl arene (**1l**), were tolerated as well. Furthermore, carbamate (**1m**) and malonate (**1n**) react efficiently. Tertiary alkyl fluorides (**1o** and **1p**) afforded the corresponding hydrogenated product **2o** and **2p** albeit in low to moderate yields. Moreover, the defluoriantion of natural product-derived compounds (**1q**, **1s**, and **1t**) proceeded smoothly, yielding the corresponding products **2q–2t** in good yields.

Table 2. Substrate scope for defluorinative hydrogenation[a]

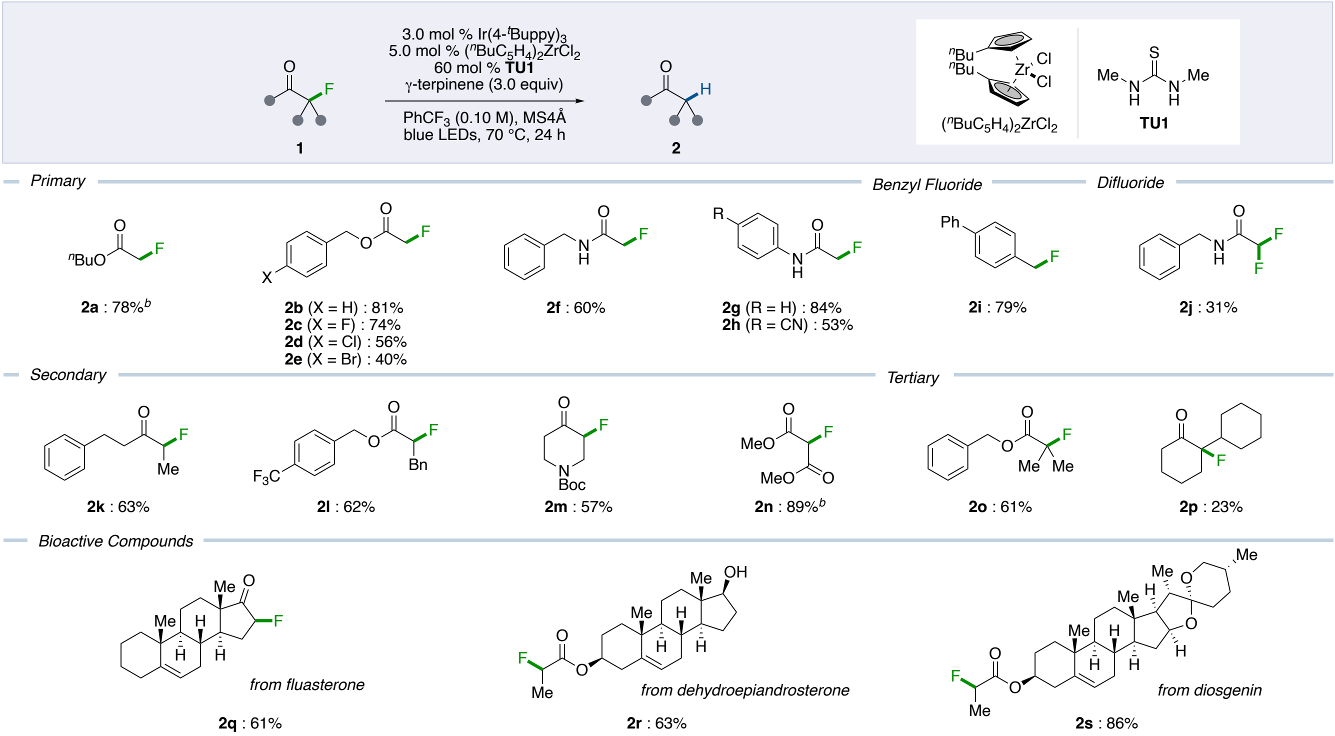

[a]Conditions: **1** (0.20 mmol), 3.0 mol % Ir(4-ᵗBuppy)$_3$, 5.0 mol % (^{n}BuC$_5$H$_4$)$_2$ZrCl$_2$, 60 mol % **TU1**, γ-terpinene (3.0 equiv), PhCF$_3$ (2.0 mL), 456 nm LEDs (Kessil Lamp), 70 °C, 24 h. All data are the average of two experiments. [b]Yields were determined by GC analysis due to its volatility. The structure of the starting materials is shown.

To further explore the synthetic potential of this reaction, we then investigated the radical alkylation of monofluorides (Table 3). After screening various conditions, we found that the combination of Ir(4-ᵗBuppy)$_3$, (^{n}BuC$_5$H$_4$)$_2$ZrCl$_2$, **TU1**, and 1,4-cyclohexadiene (1,4-CHD), under visible light irradiation efficiently converted **1b** and alkene **3** into the desired alkylated products **4**. Gratifyingly, various terminal olefins containing different functional groups, such as alkyl (**3a** and **3b**), silyl (**3c**), boronate (**3d**), and nitrile (**3e**) were all tolerated, yielding the corresponding alkylated products **4ba–4be** in moderate to good yields. Additionally, the thioglycoside derivative (**3f**), aryl benzoate (**3g**), and benzamide (**3h**) react well without affecting these reactive functional groups. Notably, even an internal alkene (**3i**) was successfully alkylated. Furthermore, activated alkenes such as enol ethers (**3j** and **3k**), enamine (**3l**), vinyl sulfide (**3m**), and indene (**3n**) afforded the corresponding alkylated products **4bi–4bn** in moderate to good yields. Interestingly, when diphenyl ethylene (**3o**) was employed, unsaturated ester **4bo** was obtained, likely via an oxidative radical-polar crossover followed by deprotonation. Furthermore, natural products and pharmaceutical compound, including safrole (**3p**), eugenol (**3q**), and alibendol (**3r**), were successfully applied in this transformation. Next, we examined the scope of fluorides using terminal alkene **3s**. α-Fluoroacetates (**1a** and **1c**) were applicable to yield the corresponding alkylated products **4as** and **4cs** in moderate yields. Amide (**1f**) and anilides (**1g** and **1h**) were also tolerated under these conditions. Moreover, malonate (**1n**) was successfully alkylated, providing product **4ns**. These results demonstrate the mild conditions of our catalytic system, which enables defluorinative alkylation to proceed efficiently with a broad range of functional groups, highlighting the versatility and unique radical reactivity of this methodology.

We then turned our attention to the reaction mechanism. First, we carried out Stern–Volmer quenching experiments (Figure 2A). Whereas dimethylthiourea (**TU1**) did not quench the excited photocatalyst Ir(4-ᵗBuppy)$_3$ (K_{SV} = –0.99), the zirconocene catalyst quenched the excited photocatalyst in a concentration-dependent manner (K_{SV} = 11). Notably, the addition of thiourea accelerated the quenching (K_{SV} = 25), supporting the role of thiourea as a zirconocene activator, consistent with our previous work.[81] Next, we conducted a radical clock experiment with β-pinene (Figure 2B). The alkylation of **1b** using β-pinene afforded the ring-opening product **4bt** in a good yield, providing strong evidence for a radical mechanism.

To determine whether the defluorination proceeds via a SET or XAT mechanism, we compared our system with Molander's SET-based defluorination of trifluoroacetamides, which is accelerated by Zn(OTf)$_2$, where zirconocene could potentially act as a Lewis acid to activate carbonyl compounds.[38,82] To explore the possibility of an SET

Table 3. Substrate scope for defluorinative alkylation[a]

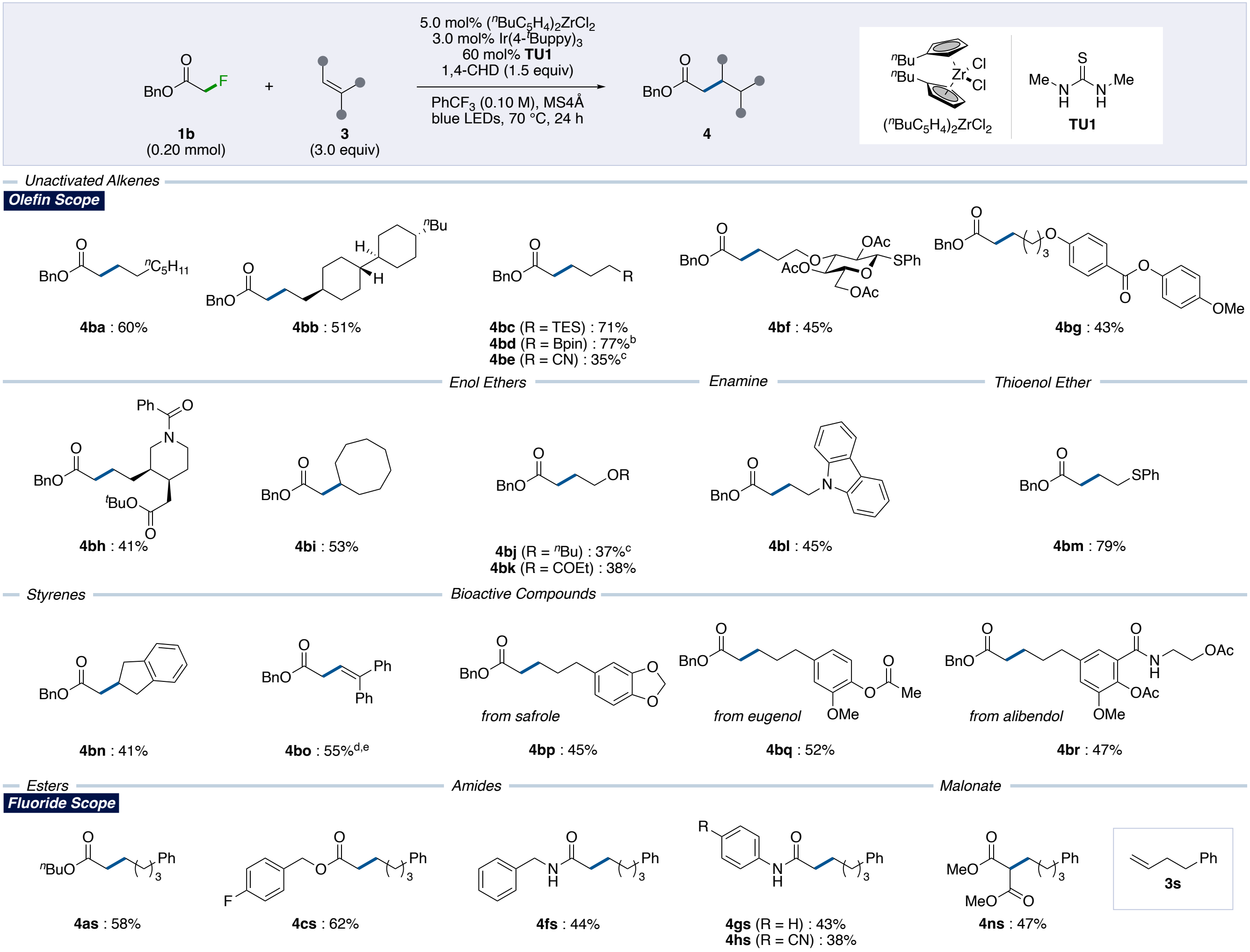

[a]Conditions: **1** (0.20 mmol), alkene **3** (3.0 equiv), 3.0 mol % Ir(4-ᵗBuppy)$_3$, 5.0 mol % (ⁿBuC$_5$H$_4$)$_2$ZrCl$_2$, 60 mol % **TU1**, 1,4-cyclohexadiene (1,4-CHD) (1.5 equiv), PhCF$_3$ (2.0 mL), 456 nm LEDs (Kessil Lamp), 70 °C, 24 h. All data are the average of two experiments. [b]Yield was determined by ^{1}H NMR using $C_2H_4Cl_2$ as an internal standard. [c]alkene (5.0 equiv) was used. [d]alkene (2.0 equiv) was used. [e]γ-terpinene (1.1 equiv) was used instead of 1,4-CHD.

pathway, we replaced zirconocene with several Lewis acids instead of zirconocene (Figure 2C). However, neither Zn(OTf)$_2$, Sc(OTf)$_2$ and BF$_3$·OEt$_2$, TMSOTf, and Cp$_2$TiCl$_2$ produced the desired product, suggesting that. zirconocene is not functioning as a Lewis acid in this case but rather as a fluorine atom abstractor. Furthermore, if the reaction followed an SET mechanism, trifluoroacetate derivatives would be expected to undergo defluorination more efficiently than monofluoroacetate derivatives due to their more favorable redox potentials (Figure 1B). To test this, we surveyed the reactivity of these fluorine-containing compounds (Figure 2D). Under our optimized conditions, trifluoroacetamide **1u** did not react, while difluoroacetamide **1t** produced the hydrogenated product in moderate yield, and monofluoroacetamide **1f** gave the product in a good yield. This reactivity trend contradicts the expectations of an SET mechanism, further supporting the XAT nature of the reaction.

Furthermore, we have conducted density functional theory (DFT) and coupled-cluster calculations at the DLPNO-RO-CCSD(T)/def2-TZVPP(D)//U-B3LYP/def2-SVP level to gain deeper insight into the reaction mechanism (Figure 2E). The reaction initiates with the coordination of α-fluoroacetate **1** to Zr^{III}, followed by the fluorine atom transfer, generating the α-carbonyl radical (**Int1**) and Zr^{IV}. The barrier of this fluorine atom transfer is estimated to be 19.4 kcal/mol. This highly exergonic process likely, driven by the strong Zr–F bond, exhibits superior irreversibility (50.8 kcal/mol) compared to previously reported XAT-type defluorinations.[18,74,75] After fluorine atom transfer, **Int1** then abstracts a hydrogen atom from 1,4-CHD to produce the hydrogenated product **2**. The calculated barrier for this HAT process is lower than the fluorine atom transfer (by 0.9–3.1 kcal/mol), suggesting that the latter is a rate-limiting step. Single-point energy calculations across various levels of theory consistently showed lower barriers for fluorine atom transfer (12.6–22.0 kcal/mol), indicating a feasible XAT process at 70 ºC (see the Supporting Information).

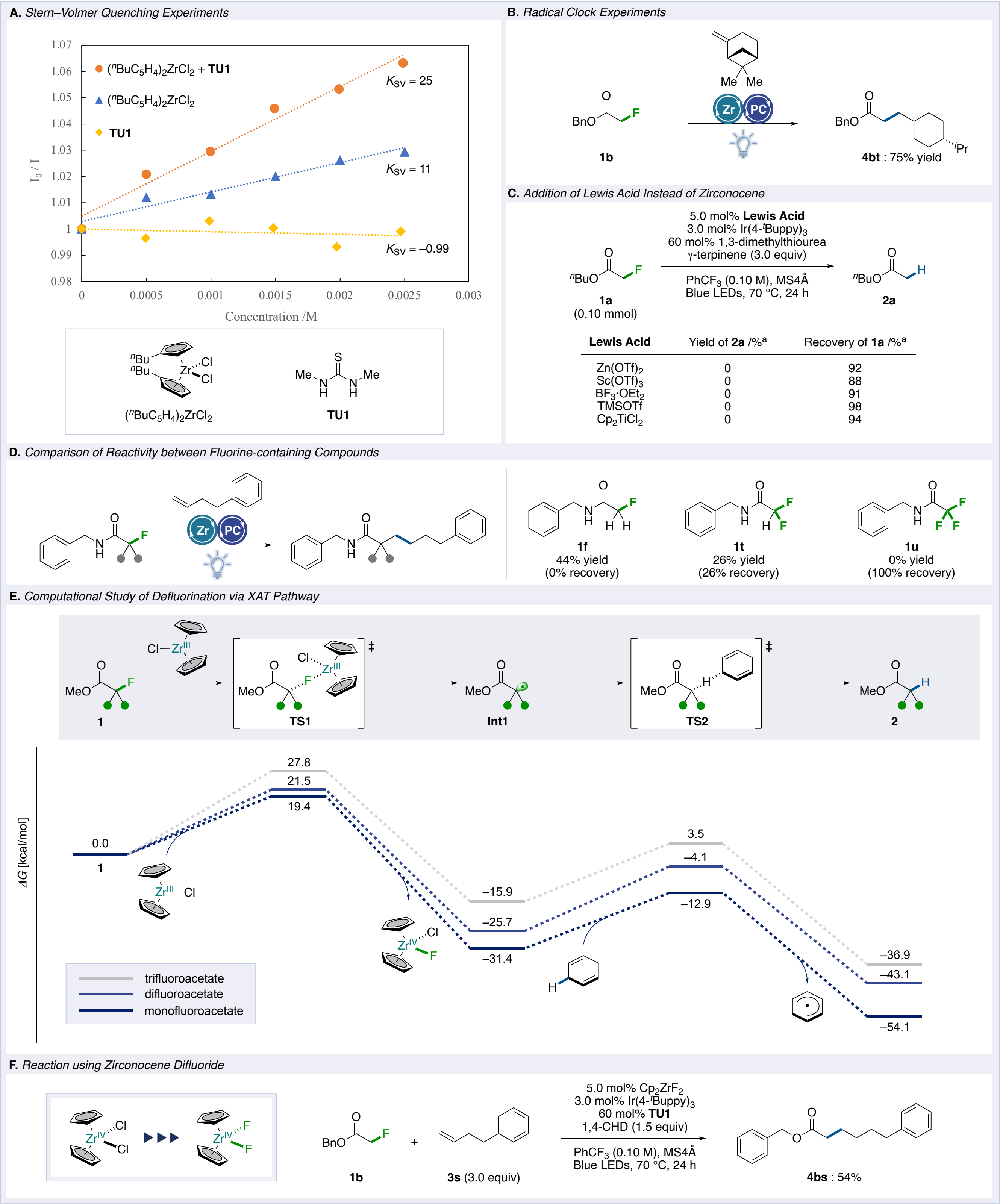

Lewis Acid	Yield of **2a** /%^{a}	Recovery of **1a** /%^{a}
Zn(OTf)$_2$	0	92
Sc(OTf)$_3$	0	88
BF$_3$·OEt$_2$	0	91
TMSOTf	0	98
Cp$_2$TiCl$_2$	0	94

Figure 2. (A) Stern–Volmer quenching experiments. (B) Radical clock experiments. (C) Comparison of the reactivity of fluorinated compounds. ^{a}Yields were determined by GC analysis using ^{n}decane as an internal standard. (D) DFT and coupled-cluster study for XAT mechanism. Potential energy calculations are performed at DLPNO-RO-CCSD(T)/def2-TZVPP(D)//U-B3LYP/def2-SVP.

Additionally, we examined the defluorination of other fluorinated compounds, such as difluoroacetate and trifluoroacetate, to confirm the reactivity trend. The activation barrier for the XAT of difluoroacetate was slightly higher (21.5 kcal/mol), it was prohibitively higher trifluoroacetate (27.8 kcal/mol) compared to monofluoroacetate. These computational results are aligned with our experimental observations (Table 2 and Figure 2D), reinforcing the XAT nature of this defluorination process. Notably, the reduction of carbonyl by Zr^{III} followed by a 1,2-fluorine shift is also a viable reaction pathway (see the Supporting Information). In this scenario, 1,2-fluorine shift is likely the rate-limiting step, with slightly higher barrier (20.0 kcal/mol) than the XAT pathway.

Lastly, we explored the possibility of ligand exchange during the reaction (Figure 2E). To investigate whether fluorinated zirconocene forms during the reaction, we performed defluorinative alkylation of monofluoroacetate **1b** using independently prepared Cp_2ZrF_2. The experimental result suggested that even if the ligand exchange occurs, the reaction proceeds without disruption to the catalytic cycle.

Based on these experimental and computational results, the proposed mechanism is outlined in Figure 3. The reaction begins with the reduction of Zr^{IV} to Zr^{III} by an excited photocatalyst. This is followed by a fluorine atom transfer from the α-fluorocarbonyl, generating an α-carbonyl radical. The α-carbonyl radical then abstracts a hydrogen atom from γ-terpinene to produce the hydrogenated product and terpinenyl radical. The terpinenyl radical is subsequently oxidized by Ir^{IV}, forming a cation and regenerating the photocatalyst. Finally, the chloride or fluoride anion produced by the reduction of Zr^{IV} deprotonate the terpinenyl cation, completing the catalytic cycle.

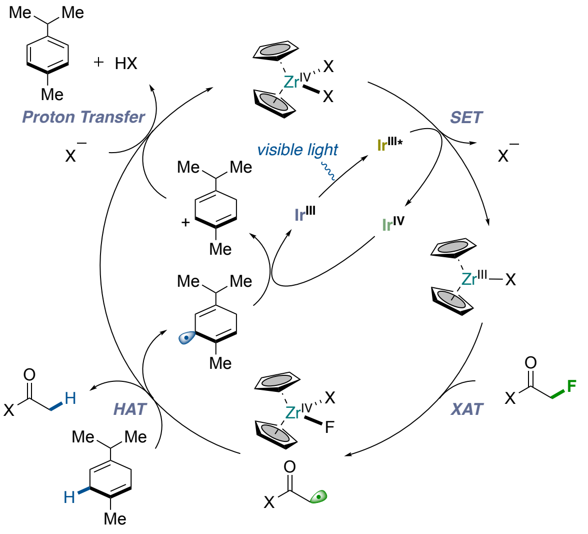

Figure 3. Proposed catalytic cycle.

CONCLUSION

In conclusion, we have developed an unprecedented fluorine atom transfer using zirconocene and photoredox catalysis. While most recent photoinduced defluorination reactions proceeded via an SET mechanism, our protocol likely operates through an XAT mechanism. This approach enables the selective removal of fluorine atom without affecting more easily reducible functional groups, such as bromoarenes, chloroarenes, and trifluoromethyl groups, positioning it as a complementary alternative to SET-based defluorination strategies. Moreover, this defluorination can be extended beyond simple hydrogenation to include alkylation, highlighting the potential of fluorine as a versatile protecting group in the synthesis of bioactive compounds. Further studies on defluorinative functionalization and expanding the substrate scope are currently underway in our laboratory.

ASSOCIATED CONTENT

Supporting Information

Experimental procedures and spectroscopic data for compounds including ^{1}H, ^{13}C, and ^{19}F spectra (PDF)

AUTHOR INFORMATION

Corresponding Authors

* Eisuke Ota – Waseda Institute for Advanced Study, Waseda University, Tokyo 162-0041, Japan;
orcid.org/0000-0002-3436-9768; Email: eota@aoni.waseda.jp
* Junichiro Yamaguchi – Department of Applied Chemistry, Waseda University, 513 Wasedatsurumakicho, Shinjuku, Tokyo 162-0041, Japan;
orcid.org/0000-0002-3896-5882; Email: junyamaguchi@waseda.jp

Authors

Haruki Takimoto – Department of Applied Chemistry, Waseda University, 513 Wasedatsurumakicho, Shinjuku, Tokyo 162-0041, Japan
Kazuhiro Aida – Department of Applied Chemistry, Waseda University, 513 Wasedatsurumakicho, Shinjuku, Tokyo 162-0041, Japan
Yoshio Nishimoto – Graduate School of Science, Kyoto University, Kyoto 606-8502, Japan
orcid.org/0000-0001-5581-4712
Daisuke Yokogawa – Graduate School of Arts and Sciences, The University of Tokyo, 3-8-1 Komaba, Meguro-ku, Tokyo 153-8902, Japan
orcid.org/0000-0002-7574-0965

ACKNOWLEDGMENT

This work was supported by JSPS KAKENHI Grant Numbers JP21H05213 (Digi-TOS) (to J.Y.), Daiichi Kigenso Kagaku Kogyo (to E.O.), and Satomi Foundation (to E.O.). This work was partly supported by JST ERATO Grant No. JPMJER1901 (to J.Y.). Materials Characterization Central Laboratory in Waseda University is acknowledged for the support of NMR and HRMS measurement. We acknowledge Kessil Lighting for the lights used in this study.

REFERENCES

(1) Gillis, E. P.; Eastman, K. J.; Hill, M. D.; Donnelly, D. J.; Meanwell, N. A. Applications of Fluorine in Medicinal Chemistry. *J. Med. Chem.* **2015**, *58*, 8315–8359.
(2) O'hagan, D. Understanding Organofluorine Chemistry. An Introduction to the C–F Bond. *Chem. Soc. Rev.* **2008**, *37*, 308–319.
(3) Trang, B.; Li, Y.; Xue, X. S.; Ateia, M.; Houk, K. N.; Dichtel, W. R. Low-Temperature Mineralization of Perfluorocarboxylic Acids. *Science* **2022**, *377*, 839–845.
(4) Shilov, A. E.; Shul'pin, G. B. Activation of C–H Bonds by Metal Complexes. *Chem. Rev.* **1997**, *97*, 2879–2932.

(5) Liu, J.; Li, S.; Xu, J.; Xu, H. Recent Advance in the C–F Bond Functionalization of Trifluoromethyl Aromatic and Carbonyl Compounds. *ChemCatChem* **2024**, *16*, e202301504.

(6) Yu, Y. J.; Zhang, F. L.; Peng, T. Y.; Wang, C. L.; Cheng, J.; Chen, C.; Houk, K. N.; Wang, Y. F. Sequential C–F Bond Functionalizations of Trifluoroacetamides and Acetates via Spin-Center Shifts. *Science* **2021**, *371*, 1232–1240.

(7) Amii, H.; Uneyama, K. C–F Bond Activation in Organic Synthesis. *Chem. Rev.* **2009**, *109*, 2119–2183.

(8) Stahl, T.; Klare, H. F. T.; Oestreich, M. Main-Group Lewis Acids for C-F Bond Activation. *ACS Catal.* **2013**, *3*, 1578–1587.

(9) Shen, Q.; Huang, Y.-G.; Liu, C.; Xiao, J.-C.; Chen, Q.-Y.; Guo, Y. Review of Recent Advances in C–F Bond Activation of Aliphatic Fluorides. *J. Fluor. Chem.* **2015**, *179*, 14–22.

(10) Ahrens, T.; Kohlmann, J.; Ahrens, M.; Braun, T. Functionalization of Fluorinated Molecules by Transition-Metal-Mediated C–F Bond Activation To Access Fluorinated Building Blocks. *Chem. Rev.* **2015**, *115*, 931–972.

(11) Fujita, T.; Fuchibe, K.; Ichikawa, J. Transition-Metal-Mediated and -Catalyzed C–F Bond Activation by Fluorine Elimination. *Angew. Chem., Int. Ed.* **2019**, *58*, 390–402.

(12) Nishimoto, Y.; Sugihara, N.; Yasuda, M. C(sp^3)–F Bond Transformation of Perfluoroalkyl Compounds Mediated by Visible-Light Photocatalysis: Spin-Center Shifts and Radical/Polar Crossover Processes via Anionic Intermediates. *Synth.* **2022**, *54*, 2765–2777.

(13) Gong, X.; Zhou, Q.; Yan, G. Recent Advances in C–F Bond Activation of Trifluoromethylated Carbonyl Compounds and Derivatives. *Org. Biomol. Chem.* **2022**, *20*, 5365–5376.

(14) Hooker, L. V.; Bandar, J. S. Synthetic Advantages of Defluorinative C–F Bond Functionalization. *Angew. Chem., Int. Ed.* **2023**, *62*, e202308880.

(15) Chen, K.; Berg, N.; Gschwind, R.; König, B. Selective Single C(sp^3)–F Bond Cleavage in Trifluoromethylarenes: Merging Visible-Light Catalysis with Lewis Acid Activation. *J. Am. Chem. Soc.* **2017**, *139*, 18444–18447.

(16) Luo, Y. C.; Tong, F. F.; Zhang, Y.; He, C. Y.; Zhang, X. Visible-Light-Induced Palladium-Catalyzed Selective Defluoroarylation of Trifluoromethylarenes with Arylboronic Acids. *J. Am. Chem. Soc.* **2021**, *143*, 13971–13979.

(17) Sugihara, N.; Suzuki, K.; Nishimoto, Y.; Yasuda, M. Photoredox-Catalyzed C–F Bond Allylation of Perfluoroalkylarenes at the Benzylic Position. *J. Am. Chem. Soc.* **2021**, *143*, 9308–9313.

(18) Kynman, A. E.; Elghanayan, L. K.; Desnoyer, A. N.; Yang, Y.; Sévery, L.; Di Giuseppe, A.; Tilley, T. D.; Maron, L.; Arnold, P. L. Controlled Monodefluorination and Alkylation of C(sp^3)-F Bonds by Lanthanide Photocatalysts: Importance of Metal-Ligand Cooperativity. *Chem. Sci.* **2022**, *13*, 14090–14100.

(19) Wang, T.; Zong, Y. Y.; Huang, T.; Jin, X. L.; Wu, L. Z.; Liu, Q. Photocatalytic Redox-Neutral Selective Single C(sp^3)–F Bond Activation of Perfluoroalkyl Iminosulfides with Alkenes and Water. *Chem. Sci.* **2023**, *14*, 11566–11572.

(20) Huang, J.; Gao, Q.; Zhong, T.; Chen, S.; Lin, W.; Han, J.; Xie, J. Photoinduced Copper-Catalyzed C–N Coupling with Trifluoromethylated Arenes. *Nat. Commun.* **2023**, *14*, 1–11.

(21) Ghosh, S.; Qu, Z. W.; Roy, S.; Grimme, S.; Chatterjee, I. Photoredox Catalyzed Single C–F Bond Activation of Trifluoromethyl Ketones: A Solvent Controlled Divergent Access of Gem-Difluoromethylene Containing Scaffolds. *Chem. Eur. J.* **2023**, *29*, 2–11.

(22) Wang, H.; Jui, N. T. Catalytic Defluoroalkylation of Trifluoromethylaromatics with Unactivated Alkenes. *J. Am. Chem. Soc.* **2018**, *140*, 163–166.

(23) Vogt, D. B.; Seath, C. P.; Wang, H.; Jui, N. T. Selective C–F Functionalization of Unactivated Trifluoromethylarenes. *J. Am. Chem. Soc.* **2019**, *141*, 13203–13211.

(24) Sap, J. B. I.; Straathof, N. J. W.; Knauber, T.; Meyer, C. F.; Meyer, C. F.; Médebielle, M.; Buglioni, L.; Genicot, C.; Trabanco, A. A.; Noël, T.; Am Ende, C. W.; Gouverneur, V. Organophotoredox Hydrodefluorination of Trifluoromethylarenes with Translational Applicability to Drug Discovery. *J. Am. Chem. Soc.* **2020**, *142*, 9181–9187.

(25) Yan, S. S.; Liu, S. H.; Chen, L.; Bo, Z. Y.; Jing, K.; Gao, T. Y.; Yu, B.; Lan, Y.; Luo, S. P.; Yu, D. G. Visible-Light Photoredox-Catalyzed Selective Carboxylation of C(sp^3)–F Bonds with CO$_2$. *Chem* **2021**, *7*, 3099–3113.

(26) Campbell, M. W.; Polites, V. C.; Patel, S.; Lipson, J. E.; Majhi, J.; Molander, G. A. Photochemical C–F Activation Enables Defluorinative Alkylation of Trifluoroacetates and -Acetamides. *J. Am. Chem. Soc.* **2021**, *143*, 19648–19654.

(27) Liu, C.; Li, K.; Shang, R. Arenethiolate as a Dual Function Catalyst for Photocatalytic Defluoroalkylation and Hydrodefluorination of Trifluoromethyls. *ACS Catal.* **2022**, *12*, 4103–4109.

(28) Liu, C.; Shen, N.; Shang, R. Photocatalytic Defluoroalkylation and Hydrodefluorination of Trifluoromethyls Using *O*-Phosphinophenolate. *Nat. Commun.* **2022**, *13*, 1–8.

(29) Shreiber, S. T.; Granados, A.; Matsuo, B.; Majhi, J.; Campbell, M. W.; Patel, S.; Molander, G. A. Visible-Light-Induced C–F Bond Activation for the Difluoroalkylation of Indoles. *Org. Lett.* **2022**, *24*, 8542–8546.

(30) Ye, J. H.; Bellotti, P.; Heusel, C.; Glorius, F. Photoredox-Catalyzed Defluorinative Functionalizations of Polyfluorinated Aliphatic Amides and Esters. *Angew. Chem., Int. Ed.* **2022**, *61*, e202115456.

(31) Wang, J.; Wang, Y.; Liang, Y.; Zhou, L.; Liu, L.; Zhang, Z. Late-Stage Modification of Drugs via Alkene Formal Insertion into Benzylic C−F Bond. *Angew. Chem., Int. Ed.* **2023**, *62*. e202215062.

(32) Xu, J.; Liu, J. W.; Wang, R.; Yang, J.; Zhao, K. K.; Xu, H. J. Construction of C–X (X = S, O, Se) Bonds via Lewis Acid-Promoted Functionalization of Trifluoromethylarenes. *ACS Catal.* **2023**, *13*, 7339–7346.

(33) Matsuo, B.; Majhi, J.; Granados, A.; Sharique, M.; Martin, R. T.; Gutierrez, O.; Molander, G. A. Transition Metal-Free Photochemical C–F Activation for the Preparation of Difluorinated-Oxindole Derivatives. *Chem. Sci.* **2023**, *14*, 2379–2385.

(34) Du, F. M.; Yan, L. Y.; Fu, M. C. Metal-Free Photoinduced Defluorinative Carboxylation of Trifluoromethylalkenes with Formate. *Eur. J. Org. Chem.* **2023**, *26*, e202300883.

(35) Min, S. Y.; Song, H. X.; Yan, S. S.; Yuan, R.; Ye, J. H.; Wang, B. Q.; Gui, Y. Y.; Yu, D. G. Photocatalytic Defluorocarboxylation Using Formate Salts as Both a Reductant and a Carbon Dioxide Source. *Green Chem.* **2023**, *25*, 6194–6199.

(36) Huang, Y.; Wan, Y. C.; Shao, Y.; Zhan, L. W.; Li, B. D.; Hou, J. Catalyst-Free Defluorinative Alkylation of Trifluoromethyls. *Green Chem.* **2023**, *25*, 8280–8285.

(37) Wang, B.; Wang, C. T.; Li, X. S.; Sun, W. H.; Liu, X. Y.; Liang, Y. M. Visible-Light-Mediated C-F Bond Cleavage for the Synthesis of Polyfluorinated Compounds. *Org. Chem. Front.* **2023**, *10*, 3341–3346.

(38) Fan, Y.; Huang, Z.; Lu, Y.; Zhu, S.; Chu, L. Defluorinative Alkylboration of Alkenes Enabled by Dual Photoredox and Copper Catalysis. *Angew. Chem., Int. Ed.* **2024**, *63*, e202315974.

(39) Jia, J.; Murugesan, K.; Zhu, C.; Yue, H.; Lee, S.-C.; Rueping, M. Multiphoton Photoredox Catalysis Enables Selective Hydrodefluorinations. *Chinese Chem. Lett.* **2024**, 109866.

(40) Jiang, Y.; Han, C.; Guo, Z.; Dai, Z.; Liang, G.; Guo, S.; Szymczak, N. K.; Tang, P. A General Photocatalytic Hydrodefluorination and Defluoroalkylation of Electronically-Variable ArCF$_3$ by Changing Commercially-Available Arenethiolates. *Green Chem.* **2024**, *26*, 4518–4527.

(41) Chen, M.; Cui, Y.; Chen, X.; Shang, R.; Zhang, X. C–F Bond Activation Enables Synthesis of Aryl Difluoromethyl Bicyclopentanes as Benzophenone-Type Bioisosteres. *Nat. Commun.* **2024**, *15*. https://doi.org/10.1038/s41467-023-44653-6.

(42) Yuan, Z. H.; Xin, H.; Gao, Y.; Sun, G. W.; Zhao, R. Y.; Duan, X. H.; Guo, L. N. Photoredox-Catalyzed Selective Deuterodefluorination of α,α-Difluoroarylacetic Esters and Amides. *Org. Chem. Front.* **2024** *11*, 4479-4486.

(43) Sun, R.; Li, G.; Xie, F.; Zhang, Q.; Sun, Y.-J.; Dai, W. Exhaustive Hydrodefluorination or Deuterodefluorination of Trifluoromethylarenes via Metal-Free Photoredox Catalysis. *Org. Lett.* **2024**, *26*, 928–932.

(44) Luo, Y.-R. *Comprehensive Handbook of Chemical Bond Energies*; Luo, Y.-R., Ed.; CRC Press: Boca Raton, 2007.

(45) Juliá, F. New Synthetic Strategies Based on Photoinduced Halogen-Atom Transfer (XAT). In *Photochemistry*; Crespi, S., Protti, S., Eds.; Royal Society of Chemistry, 2023; pp 361–383.

(46) Juliá, F.; Constantin, T.; Leonori, D. Applications of Halogen-Atom Transfer (XAT) for the Generation of Carbon Radicals in Synthetic Photochemistry and Photocatalysis. *Chem. Rev.* **2022**, *122*, 2292–2352.

(47) Ji, C. L.; Zhai, X.; Fang, Q. Y.; Zhu, C.; Han, J.; Xie, J. Photoinduced Activation of Alkyl Chlorides. *Chem. Soc. Rev.* **2023**, *52*, 6120–6138.

(48) Constantin, T.; Juliá, F.; Sheikh, N. S.; Leonori, D. A Case of Chain Propagation: α-Aminoalkyl Radicals as Initiators for Aryl Radical Chemistry. *Chem. Sci.* **2020**, *11*, 12822–12828.

(49) Constantin, T.; Zanini, M.; Regni, A.; Sheikh, N. S.; Juliá, F.; Leonori, D. Aminoalkyl Radicals as Halogen-Atom Transfer Agents for Activation of Alkyl and Aryl Halides. *Science* **2020**, *367*, 1021–1026.

(50) Zhao, H.; McMillan, A. J.; Constantin, T.; Mykura, R. C.; Juliá, F.; Leonori, D. Merging Halogen-Atom Transfer (XAT) and Cobalt Catalysis to Override E2-Selectivity in the Elimination of Alkyl Halides: A Mild Route Towardcontra-Thermodynamic Olefins. *J. Am. Chem. Soc.* **2021**, *143*, 14806–14813.

(51) Górski, B.; Barthelemy, A. L.; Douglas, J. J.; Juliá, F.; Leonori, D. Copper-Catalysed Amination of Alkyl Iodides Enabled by Halogen-Atom Transfer. *Nat. Catal.* **2021**, *4*, 623–630.

(52) Zhang, Z.; Górski, B.; Leonori, D. Merging Halogen-Atom Transfer (XAT) and Copper Catalysis for the Modular Suzuki-Miyaura-Type Cross-Coupling of Alkyl Iodides and Organoborons. *J. Am. Chem. Soc.* **2022**, *144*, 1986–1992.

(53) Kostromitin, V. S.; Sorokin, A. O.; Levin, V. V.; Dilman, A. D. Aminals as Powerful XAT-Reagents: Activation of Fluorinated Alkyl Chlorides. *Chem. Sci.* **2023**, *14*, 3229–3234.

(54) Zhang, P.; Le, C. C.; MacMillan, D. W. C. Silyl Radical Activation of Alkyl Halides in Metallaphotoredox Catalysis: A Unique Pathway for Cross-Electrophile Coupling. *J. Am. Chem. Soc.* **2016**, *138*, 8084–8087.

(55) Smith, R. T.; Zhang, X.; Rincón, J. A.; Agejas, J.; Mateos, C.; Barberis, M.; García-Cerrada, S.; De Frutos, O.; Macmillan, D. W. C. Metallaphotoredox-Catalyzed Cross-Electrophile Csp^3-Csp^3 Coupling of Aliphatic Bromides. *J. Am. Chem. Soc.* **2018**, *140*, 17433–17438.

(56) Liu, W.; Lavagnino, M. N.; Gould, C. A.; Alcázar, J.; MacMillan, D. W. C. A Biomimetic S_H2 Cross-Coupling Mechanism for Quaternary sp^3-Carbon Formation. *Science* **2021**, *374*, 1258–1263.

(57) Luridiana, A.; Mazzarella, D.; Capaldo, L.; Rincón, J. A.; García-Losada, P.; Mateos, C.; Frederick, M. O.; Nuño, M.; Jan Buma, W.; Noël, T. The Merger of Benzophenone HAT Photocatalysis and Silyl Radical-Induced XAT Enables Both Nickel-Catalyzed Cross-Electrophile Coupling and 1,2-Dicarbofunctionalization of Olefins. *ACS Catal.* **2022**, *12*, 11216–11225.

(58) Garry, O. L.; Heilmann, M.; Chen, J.; Liang, Y.; Zhang, X.; Ma, X.; Yeung, C. S.; Bennett, D. J.; MacMillan, D. W. C. Rapid Access to 2-Substituted Bicyclo[1.1.1]Pentanes. *J. Am. Chem. Soc.* **2023**, *145*, 3092–3100.

(59) Gould, C. A.; Pace, A. L.; MacMillan, D. W. C. Rapid and Modular Access to Quaternary Carbons from Tertiary Alcohols via Bimolecular Homolytic Substitution. *J. Am. Chem. Soc.* **2023**, *145*, 16330–16336.

(60) Chen, T. Q.; MacMillan, D. W. C. A Metallaphotoredox Strategy for the Cross-Electrophile Coupling of α-Chloro Carbonyls with Aryl Halides. *Angew. Chem., Int. Ed.* **2019**, *58*, 14584–14588.

(61) Kornfilt, D. J. P.; Macmillan, D. W. C. Copper-Catalyzed Trifluoromethylation of Alkyl Bromides. *J. Am. Chem. Soc.* **2019**, *141*, 6853–6858.

(62) Lovett, G. H.; Chen, S.; Xue, X. S.; Houk, K. N.; MacMillan, D. W. C. Open-Shell Fluorination of Alkyl Bromides: Unexpected Selectivity in a Silyl Radical-Mediated Chain Process. *J. Am. Chem. Soc.* **2019**, *141*, 20031–20036.

(63) Lavagnino, M. N.; Liang, T.; MacMillan, D. W. C. HARC as an Open-Shell Strategy to Bypass Oxidative Addition in Ullmann-Goldberg Couplings. *Proc. Natl. Acad. Sci. U. S. A.* **2020**, *117*, 21058–21064.

(64) Sakai, H. A.; Liu, W.; Le, C. "Chip"; MacMillan, D. W. C. Cross-Electrophile Coupling of Unactivated Alkyl Chlorides. *J. Am. Chem. Soc.* **2020**, *142*, 11691–11697.

(65) Zhao, X.; MacMillan, D. W. C. Metallaphotoredox Perfluoroalkylation of Organobromides. *J. Am. Chem. Soc.* **2020**, *142*, 19480–19486.

(66) Dow, N. W.; Cabré, A.; MacMillan, D. W. C. A General N-Alkylation Platform via Copper Metallaphotoredox and Silyl Radical Activation of Alkyl Halides. *Chem* **2021**, *7*, 1827–1842.

(67) Pipal, R. W.; Stout, K. T.; Musacchio, P. Z.; Ren, S.; Graham, T. J. A.; Verhoog, S.; Gantert, L.; Lohith, T. G.; Schmitz, A.; Lee, H. S.; Hesk, D.; Hostetler, E. D.; Davies, I. W.; MacMillan, D. W. C. Metallaphotoredox Aryl and Alkyl Radiomethylation for PET Ligand Discovery. *Nature* **2021**, *589*, 542–547.

(68) Zhang, Z. Q.; Sang, Y. Q.; Wang, C. Q.; Dai, P.; Xue, X. S.; Piper, J. L.; Peng, Z. H.; Ma, J. A.; Zhang, F. G.; Wu, J. Difluoromethylation of Unactivated Alkenes Using Freon-22 through Tertiary Amine-Borane-Triggered Halogen Atom Transfer. *J. Am. Chem. Soc.* **2022**, *144*, 14288–14296.

(69) Wan, T.; Capaldo, L.; Ravelli, D.; Vitullo, W.; de Zwart, F. J.; de Bruin, B.; Noël, T. Photoinduced Halogen-Atom Transfer by *N*-Heterocyclic Carbene-Ligated Boryl Radicals for $C(sp^3)$-$C(sp^3)$ Bond Formation. *J. Am. Chem. Soc.* **2023**, *145*, 991–999.

(70) Zhang, Z.; Poletti, L.; Leonori, D. A Radical Strategy for the Alkylation of Amides with Alkyl Halides by Merging Boryl Radical-Mediated Halogen-Atom Transfer and Copper Catalysis. *J. Am. Chem. Soc.* **2024**, *146*, 22424–22430.

(71) Zhang, Z.; Tilby, M. J.; Leonori, D. Boryl Radical-Mediated Halogen-Atom Transfer Enables Arylation of Alkyl Halides with Electrophilic and Nucleophilic Coupling Partners. *Nat. Synth.* **2024**. https://doi.org/10.1038/s44160-024-00587-5.

(72) Constantin, T.; Górski, B.; Tilby, M. J.; Chelli, S.; Juliá, F.; Llaveria, J.; Gillen, K. J.; Zipse, H.; Lakhdar, S.; Leonori, D. Halogen-Atom and Group Transfer Reactivity Enabled by Hydrogen Tunneling. *Science.* **2022**, *377*, 1323–1328.

(73) Caiger, L.; Sinton, C.; Constantin, T.; Douglas, J. J.; Sheikh, N. S.; Juliá, F.; Leonori, D. Radical Hydroxymethylation of Alkyl Iodides Using Formaldehyde as a C1 Synthon. *Chem. Sci.* **2021**, *12*, 10448–10454.

(74) Kostromitin, V. S.; Sorokin, A. O.; Levin, V. V.; Dilman, A. D. C–F Activation of Fluorinated Esters Using Photocatalytically Generated Diaminoalkyl Radical. *Org. Lett.* **2023**, *25*, 6598–6602.

(75) Koo, J.; Kim, W.; Jhun, B. H.; Park, S.; Song, D.; You, Y.; Lee, H. G. Halogen Atom Transfer-Induced Homolysis of C–F Bonds by the Excited-State Boryl Radical. *J. Am. Chem. Soc.* **2024**, *146*, 22874–22880.

(76) Okita, T.; Aida, K.; Tanaka, K.; Ota, E.; Yamaguchi, J. Chlorine Atom Transfer of Unactivated Alkyl Chlorides Enabled by Zirconocene and Photoredox Catalysis. *Precis. Chem.* **2023**, *1*, 112–118.

(77) Kraft, B. M.; Lachicotte, R. J.; Jones, W. D. Aliphatic Carbon−Fluorine Bond Activation Using $(C_5Me_5)_2ZrH_2$. *J. Am. Chem. Soc.* **2000**, *122*, 8559–8560.

(78) Kraft, B. M.; Lachicotte, R. J.; Jones, W. D. Aliphatic and Aromatic Carbon-Fluorine Bond Activation with $Cp*_2ZrH_2$: Mechanisms of Hydrodefluorination. *J. Am. Chem. Soc.* **2001**, *123*, 10973–10979.

(79) Zachmanoglou, C. E.; Docrat, A.; Bridgewater, B. M.; Parkin, G.; Brandow, C. G.; Bercaw, J. E.; Jardine, C. N.; Lyall, M.;

Green, J. C.; Keister, J. B. The Electronic Influence of Ring Substituents and Ansa Bridges in Zirconocene Complexes as Probed by Infrared Spectroscopic, Electrochemical, and Computational Studies. *J. Am. Chem. Soc.* **2002**, *124*, 9525–9546.

(80) Lambert, F. L.; Ingall, G. B. Voltammetry of Organic Halogen Compounds. IV. The Reduction of Organic Chlorides at the Vitreous (Glassy) Carbon Electrode. *Tetrahedron Lett.* **1974**, *15*, 3231–3234.

(81) Aida, K.; Hirao, M.; Funabashi, A.; Sugimura, N.; Ota, E.; Yamaguchi, J. Catalytic Reductive Ring Opening of Epoxides Enabled by Zirconocene and Photoredox Catalysis. *Chem* **2022**, *8*, 1762–1774.

(82) Fukuzumi, S.; Jung, J.; Lee, Y. M.; Nam, W. Effects of Lewis Acids on Photoredox Catalysis. *Asian J. Org. Chem.* **2017**, *6*, 397–409.

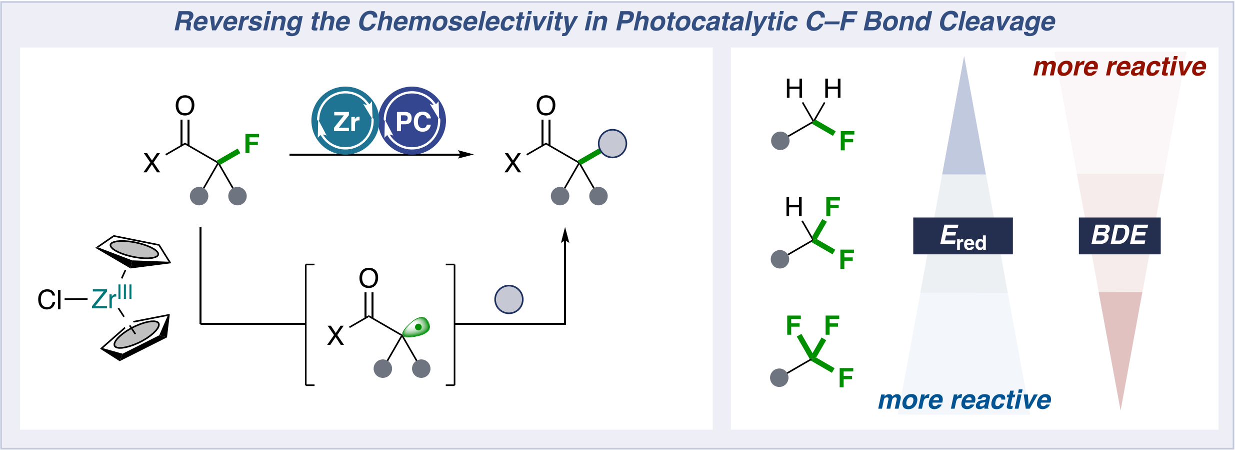
Reversing the Chemoselectivity in Photocatalytic C–F Bond Cleavage
O
X
F
Zr
PC
Cl
Zr^{III}
H H
H F
F F
E_{red}
BDE
more reactive
more reactive